THE JOURNAL OF PHYSICAL CHEMISTRY B

Article

pubs.acs.org/JPCB

Ewald Summation Approach to Potential Models of Aqueous Electrolytes Involving Gaussian Charges and Induced Dipoles: Formal and Simulation Results

Ariel A. Chialvo*[,†] and Lukas Vlcek[†,‡]

[†]Chemical Sciences Division, Geochemistry & Interfacial Sciences Group, Oak Ridge National Laboratory, Oak Ridge, Tennessee 37831-6110, United States

[‡]Joint Institute for Computational Sciences, Oak Ridge National Laboratory, Oak Ridge, Tennessee 37831-6173, United States

Supporting Information

ABSTRACT: We present a detailed derivation of the complete set of expressions required for the implementation of an Ewald summation approach to handle the long-range electrostatic interactions of polar and ionic model systems involving Gaussian charges and induced dipole moments with a particular application to the isobaric−isothermal molecular dynamics (NPT-MD) simulation of our Gaussian charge polarizable (GCP) water model and its extension to aqueous electrolyte solutions. The set is comprised of the individual components of the potential energy, electrostatic potential, electrostatic field and gradient, electrostatic force, and corresponding virial. Moreover, we show how the derived expressions converge to known point-based electrostatic counterparts when the parameters, defining the Gaussian charge and induced dipole distributions, are extrapolated to their limiting point values. Finally, we test the simulation outcomes from the Ewald implementation against the corresponding reaction-field (RF) approach at three contrasting hydrogen-bonded water environments, including thermodynamic quantities, polarization behavior, and microstructural properties, where the simulated microstructures are compared with the available neutron scattering and X-ray diffraction data.

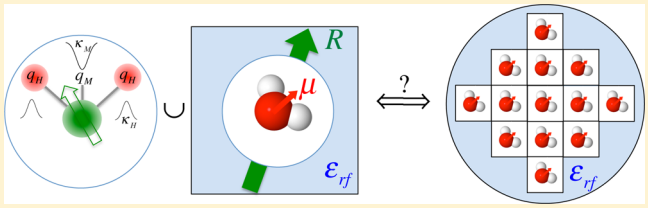

I. INTRODUCTION

The microscopic behavior of water has been traditionally described in terms of simple atomistic models comprising an arrangement of fixed point charges located either at atomic or virtual sites according to a realistic geometry similar to, or a perturbation of, that of the gas phase molecule.[1,2] The magnitude of these electrostatic charges, constrained by the molecule's electroneutrality, becomes one of the adjustable parameters used in the regression of the model's force fields, and defines the effective permanent dipole moment of the model molecule. Because the magnitude of these charges and resulting dipole moment cannot change in response to the electric field fluctuations of the surrounding environment, these models are unable to account for the significant isotropic variations of polarization caused by changes in environmental dielectric permittivity (e.g., variations of state conditions) and the anisotropic polarization response resulting from the formation of interfaces,[3] the presence of charged species,[4] and under the effect of external electric fields.[5] Typically, these *nonpolarizable* models for polar fluids involve enhanced electrostatic charges from the corresponding values describing the isolated (i.e., gas phase) permanent dipole moment.[6] Consequently, these models are usually capable of representing properly the liquid-phase branch of the orthobaric (VLE) curve but fail dramatically in the description of the corresponding vapor phase due to the *overpolarized* nature of the regressed effective permanent dipole moment.[7]

The obvious route to overcome the deficiencies of nonpolarizable models is to account explicitly for the polarization phenomena, most frequently involving point charges and polarizable point dipoles,[8−11] even though there are numerous other approaches such as polarizable point charges,[12] charge-on-spring models involving point charges,[13−16] and electronegativity equalization (a.k.a. fluctuating charge) methods.[17−19] For detailed discussions of these alternative approaches, the reader should consult the recent reviews in this matter.[10,11,20−22]

Models comprising point charges and point polarizable dipoles may however suffer from just the opposite behavior, i.e., overpolarization at short distances[23,24] and the potential occurrence of polarization catastrophe[25] driven by the inability of point charges to handle charge penetrations.[26] Early effort to deal with overpolarization and prevent the occurrence of polarization catastrophe during close encounters involved the use of damping functions to the dipole−dipole interactions,[27] a procedure that inspired new developments in the modeling of water[28] based on point charges, Gaussian charge distribu-

Received: September 8, 2014
Revised: October 31, 2014
Published: November 1, 2014

tions,[29−32] multipole expansions,[33] and the implementation of other damping functions to reduce smoothly the strength of the electrostatic interactions in close encounters.[16,34]

An effective and realistic approach to overcome over-polarization, as well as to avoid the potential occurrence of polarization catastrophe, involves the use of smeared—rather than point—charges in the modeling of electrostatics of polarizable fluids, and perhaps the first application of this approach to water modeling was done by Sprik and Klein[35] who introduced Gaussian electrostatic charges with variable magnitude to describe polarizability without invoking fluctuating point dipoles, followed soon after by Zhu et al.[36] with an alternative representation to the Gaussian distributions.

Regardless of the involvement of point or Gaussian distributed charges and/or multipoles, we still must deal with the proper evaluation of long-range electrostatic interactions in finite-size systems under periodic boundary conditions.[37] While numerous methods have been introduced to deal with this type of long-range interactions including plain spherical truncation,[38] neutralized spherical truncation plus screening,[39] shifted-force spherical truncation plus screening,[40] kubic harmonics,[41] reaction field,[42] generalized reaction field,[43] and lattice summations,[44−47] the reaction field and Ewald summation approaches are the most frequently used. In fact, following earlier developments by Ruocco et al.[48] for the consistent treatment of point-multipole polarizable systems, we tailored their center-of-mass (i.e., neutral molecule) reaction field method to deal with polarizable interactions involving Gaussian distributions (for details, see Appendix E in the Supporting Information for the current manuscript).[29]

Under the above context, the main goal of this work is to develop an Ewald summation implementation of the original reaction field Gaussian charge polarizable (GCP) water model and its extension to aqueous electrolyte solutions. For that purpose, in section II, we present and discuss the explicit full description of the interaction Hamiltonian for the GCP model because it has not been done previously, and consequently has been the source of some misrepresentations in the literature (*vide infra*). Then, in section III, we derive the Ewald summation expressions to account for the long-range electrostatic interactions, as a more advantageous alternative to the original reaction field implementation, including the individual components of the potential energy, electrostatic potential, electrostatic field and gradient, the force, and the corresponding virial. Moreover, we highlight how the derived expressions converge to known point-charge and point-dipole counterparts when the underlying Gaussian distributions become limiting Dirac-delta distributions. After discussing some simulation details about the Ewald implementation, in section IV, we illustrate its application by NPT-MD of water under three distinct extreme local environments, contrast the outcomes with the corresponding from the reaction field approach, and compare the simulated microstructures against available neutron scattering and X-ray diffraction data. We wrap up the manuscript with a summary of findings and relevant remarks.

II. GAUSSIAN CHARGES AND THE DIPOLE POLARIZABLE WATER MODEL

Back in June of 1997, during the 13th Symposium on Thermophysical Properties at the University of Colorado (Boulder), we introduced a "*Simple transferable intermolecular potential for the molecular simulation of water over wide ranges of state conditions*" comprising a few (at the time) novel modeling features, namely, the use of smeared (rather than point) partial charge distributions with corresponding induced dipole moments together with an exponential-6 (rather than the usual Lennard-Jones) potential[29] to account for the nonelectrostatic interactions. This model was partially the result of findings from our previous efforts regarding the engineering of a simple self-consistent point-dipole polarizable description of water behavior over a wide range of state conditions,[49] and motivated by the need to address some controversial issues[50] about the hydrogen bonding and microstructure of supercritical water raised by emerging neutron diffraction with isotope substitution experiments.[51−53]

The original model was subsequently reparameterized by Paricaud et al.,[31] and dubbed Gaussian charge polarizable, to describe accurately the properties of water from the gas to the condensed phases, i.e., from low density environments characterized by the first few virial coefficients,[54,55] the equilibrium configuration of small clusters,[56] the vapor−liquid surface tension,[57] and the corresponding orthobaric curve[31] to the high density close-packed phases typically encountered in extreme geological environments.[58]

The GCP water model comprises a planar rigid gas-phase geometry with three atomic masses for the oxygen (O) and hydrogen (H) sites whose O−H bonds described by l_{OH} = 0.9572 Å define the angle ∠HOH = 104.52°. Two additional sites complete the model geometry, i.e., the molecular center of mass (com) and the location of massless site (M) bearing a Gaussian electrostatic charge with a magnitude $q_M = -2q_H = -1.2226e$ at l_{OM} = 0.27 Å from the O-site along the ∠HOH bisector, resulting in a permanent dipole (gas phase) moment of 1.85 D (Figure 1 in ref 31). In terms of site−site interactions, this model comprises dispersion, Gaussian charges, and corresponding induced dipole interactions. Currently, the dispersion interactions that account for the van der Waals interactions between the oxygen sites are described by a soft-repulsive modification of the original Buckingham potential[59]

$$\phi_{buck}(r_{OO}) = \left(\frac{\varepsilon_{OO}}{1 - 6/\gamma_{OO}}\right) \times [(6/\gamma_{OO})\exp(\gamma_{OO}[1 - (r_{OO}/\sigma_{OO})]) - (\sigma_{OO}/r_{OO})^6] \quad (1)$$

rather than the original hard-core repulsive version,[29,31] to avoid potential issues[60] associated with the divergence of $\phi_{buck}(r_{OO} < r_m)$, where r_m is the smallest root of $[\partial\phi_{buck}(r_{OO})/\partial r_{OO}]_{r_{OO}=r_m} = 0$. Therefore,

$$U_{disp} = \sum_{i<j=1,N} \phi_{m\_exp6}(r_{OO}) \quad (2)$$

where the pair potential for the oxygen−oxygen interactions is given by a continuous representation described as follows

$$\phi_{m\_exp6}(r_{OO}) = \begin{cases} \phi_{buck}(r_{OO}) & \text{if } r_c > r_{OO} > r_m \\ -\phi_{buck}(r_{OO}) + 2\phi_{buck}(r_m) & \text{if } r_{OO} \le r_m \end{cases} \quad (3)$$

with γ_{OO} = 12.75, ε_{OO}/k = 110.0 K, σ_{OO} = 3.69 Å, and $r_m \cong 0.273\sigma_{OO}$ resulting from the numerical solution of the transcendental equation $\exp(\gamma_{OO}[1 - (r_m/\sigma_{OO})]) - (\sigma_{OO}/r_m)^7 = 0$, where $r_c \le 0.5L$ is the cutoff truncation radius consistent with the simulation box size L.

dx.doi.org/10.1021/jp509074p | J. Phys. Chem. B 2014, 118, 13658−13670

The total electrostatic energy of the system of Gaussian partial charges and resulting induced dipole moments can be written as follows:[61]

$$U_{el} = U_{int} + U_{pol} \tag{4}$$

where the subscripts int and pol denote interaction and polarization contributions, respectively. In particular, the int contributions can be identified as

$$U_{int} = 0.5 \sum_{i\neq j} \int_V [(\sum_\alpha \rho_{q_i^\alpha}(\mathbf{r}) + \rho_{\mu_i}(\mathbf{r}))(\sum_\beta \rho_{q_j^\beta}(\mathbf{r}') + \rho_{\mu_j}(\mathbf{r}'))/|\mathbf{r} - \mathbf{r}'|]\, d\mathbf{r}\, d\mathbf{r}' \tag{5}$$

where the partial charge distribution $\rho_{q_i^\alpha}(r)$ for the α-site partial-charge q_i^α and the center-of-mass dipole-charge distribution $\rho_{\mu_i}(r)$ for the induced dipole $\boldsymbol{\mu}_i^{ind}$ are given by the following Gaussians charge-density operators[29,62]

$$\rho_{q_i^\alpha}(r) = [q_i^\alpha/(2\pi\sigma_\alpha^2)^{1.5}] \exp[-|\mathbf{r} - \mathbf{r}_{i_\alpha}|^2/2\sigma_\alpha^2] \tag{6}$$

and

$$\rho_{\mu_i}(r) = [\boldsymbol{\mu}_i^{ind}\cdot\nabla_i/(2\pi\sigma_\mu^2)^{1.5}] \exp[-|\mathbf{r} - \mathbf{r}_i|^2/2\sigma_\mu^2] \tag{7}$$

From eq 5 follows immediately that $U_{int} = U_{qq} + U_{q\mu} + U_{\mu\mu}$, where the individual terms correspond to the charge−charge, charge−induced dipole, and induced dipole−induced dipole interactions, respectively. In fact, according to eqs 5−7, these contributions can be written as follows (see Appendix A in the Supporting Information for details):

$$U_{qq} = \sum_{i<j}\sum_{\alpha,\beta} q_i^\alpha q_j^\beta \hat{T}_{i_\alpha j_\beta}(r_{i_\alpha j_\beta}) \tag{8}$$

$$U_{q\mu} = \sum_{i<j}\sum_{\alpha,\beta} (-q_i^\alpha \hat{T}^\gamma_{i_\alpha j}(r_{i_\alpha j})\mu_j^{ind,\gamma} + \mu_i^{ind,\gamma}\hat{T}^\gamma_{ij_\beta}(r_{ij_\beta})q_j^\beta) \tag{9}$$

$$U_{\mu\mu} = \sum_{i<j} \mu_i^{ind,\alpha}\hat{T}_{ij}^{\alpha\beta}(r_{ij})\mu_j^{ind,\beta} \tag{10}$$

where the Cartesian operators $\hat{T}(r) \equiv \mathrm{erf}(\kappa r)/r$, $\hat{T}^\gamma(r) \equiv \nabla_\gamma\hat{T}(r)$, and $\hat{T}^{\gamma\lambda}(r) \equiv \nabla_\lambda\hat{T}^\gamma(r)$ are given explicitly by the following expressions:

$$\hat{T}_{i_\alpha j_\beta}(r_{i_\alpha j_\beta}) = \mathrm{erf}(\kappa_{\alpha\beta}r_{i_\alpha j_\beta})/r_{i_\alpha j_\beta} = s_0(r_{i_\alpha j_\beta})/r_{i_\alpha j_\beta} \tag{11}$$

$$\hat{T}^\gamma_{i_\alpha j}(r_{i_\alpha}) = -(r^\gamma_{i_\alpha j}/r_{i_\alpha j}^3)[\mathrm{erf}(\kappa_{\alpha\mu}r_{i_\alpha j}) - (2/\sqrt{\pi})r_{i_\alpha j}\kappa_{\alpha\mu}\exp(-\kappa_{\alpha\mu}^2 r_{i_\alpha j}^2)] = -s_1(r_{i_\alpha j})r^\gamma_{i_\alpha j}/r_{i_\alpha j}^3 \tag{12}$$

$$\hat{T}_{ij}^{\gamma\lambda}(r) = \{\mathrm{erf}(\kappa_{\mu\mu}r_{ij}) - [(2\kappa_{\mu\mu}r_{ij}/\sqrt{\pi}) + (4\kappa_{\mu\mu}^3 r_{ij}^3/3\sqrt{\pi})]\exp(-\kappa_{\mu\mu}^2 r_{ij}^2)\}3r^\gamma_{ij}r^\lambda_{ij}/r_{ij}^5 - [\mathrm{erf}(\kappa_{\mu\mu}r_{ij}) - (2\kappa_{\mu\mu}r_{ij}/\sqrt{\pi})]\delta_{\gamma\lambda}/r_{ij}^3 = s_2(r_{ij})3r^\gamma_{ij}r^\lambda_{ij}/r_{ij}^5 - s_1(r_{ij})\delta_{\gamma\lambda}/r_{ij}^3 \tag{13}$$

The superscripts γ and λ in eqs 9−13 denote Cartesian components, r_{ij} represents the center-of-mass distance between the ij-pair of molecules, $r_{i_\alpha j}$ describes the distance between the molecular site α in molecule i and the center of mass of the j molecule, $\mathrm{erf}(x) \equiv (2/\sqrt{2})\int_0^x \exp(-t)^2\, dt$ is the error function,[63] $\nabla_\gamma(\cdots) \equiv (r^\gamma/\mathbf{r})[\partial(\cdots)/\partial r]$ is the Cartesian gradient operator, $\delta_{\gamma\lambda}$ is Kronecker's delta, $\kappa_{\alpha\beta} = 1/[2(\sigma_\alpha^2 + \sigma_\beta^2)]^{1/2}$, with $\kappa_\delta = (\sigma_\delta\sqrt{2})^{-1}$ for $\delta = (\alpha, \beta, \mu, s)$, and the prefactors $s_n(r)$ are linked by the following recursive expression: $s_n(r) = s_{n-1}(r) - [r/(2n-1)][\partial s_{n-1}(r)/\partial r]$.

Finally, the polarization contribution in eq 4 resulting from the self-consistent solution of $\partial U_{el}/\partial\boldsymbol{\mu}_i^{ind} = \partial U_{el}/\partial\mathbf{E}_i^{tot} = 0$[48,64] becomes

$$U_{pol} = 0.5\sum_i (\boldsymbol{\mu}_i^{ind}\cdot\boldsymbol{\mu}_i^{ind})/\alpha_i \tag{14}$$

where the link between the induced dipole moment $\boldsymbol{\mu}_i^{ind}$ at the center of mass of the i molecule bearing a molecular polarizability α_i and the corresponding total electric field $\mathbf{E}_i^{tot} = \mathbf{E}_i^{qq} + \mathbf{E}_i^{\mu\mu}$ is given by the $\boldsymbol{\mu}_i^{ind}$-implicit expression,

$$\boldsymbol{\mu}_i^{ind} = \alpha_i\mathbf{E}_i^{tot}(\{\boldsymbol{\mu}_{i=1,N}^{ind}\}) \tag{15}$$

where we use the notation $\mathbf{E}_i^{tot}(\{\boldsymbol{\mu}_{i=1,N}^{ind}\})$ to highlight its implicit nature through $\mathbf{E}_i^{\mu\mu}(\{\boldsymbol{\mu}_{i=1,N}^{ind}\})$, whose numerical solution will be discussed in section IV.

III. EWALD SUMMATION IMPLEMENTATION

The treatment of the long-ranged electrostatic interactions in the original version of the GCP water model was based on a center-of-mass reaction field approach[48,49] that might become problematic when trying to extend the GCP model to the description of ions in solution or inhomogeneous environments such as vapor−liquid and solid−liquid interfaces.[37,65−68] For that reason here we introduce and discuss an Ewald summation implementation of a general GCP model for water and aqueous electrolytes solutions.

a. Components of the Potential Energy, Electrostatic Potential, and Field. The underlying idea behind the Ewald approach is depicted in Figure 1, and highlights the fact that the width of the Gaussian charge and induced dipole distributions in eqs 6 and 7, i.e., σ_α and σ_μ, are typically smaller than that for the standard Gaussian screening parameter σ_s; therefore, we can invoke the same ideas behind the summation method for point charges and point dipole distributions to derive the Ewald summation expressions for the corresponding Gaussian distributions. Note that the condition $\sigma_\alpha, \sigma_\mu \ll \sigma_s$ is usually a

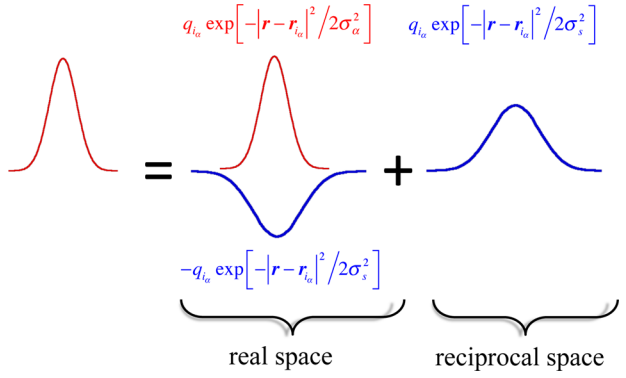

Figure 1. Schematic representation of the split between real- and reciprocal-space contributions in the Ewald summation approach involving Gaussian smeared electrostatic charges and induced dipoles.

dx.doi.org/10.1021/jp509074p | J. Phys. Chem. B 2014, 118, 13658−13670

physical constraint that allows accurate evaluation of the system's electrostatics according to the splitting into fast converging contributions from short-ranged (in real-space) and long-ranged (in reciprocal-space) interactions.[69]

For that purpose, we introduce into eq 5 an additional attenuation Gaussian function, characterized by its width σ_s, so that the resulting counterpart expressions to eqs 8−10 remain formally the same, though the $s_n(r)$ prefactors in the Cartesian operators given by eqs 11−13 now involve additional contributions from the interactions between the original Gaussian charge densities and Ewald's Gaussian screening charge distribution. The new prefactors follow a similar recursive expression as that for the case involving point-charge and point-dipole distributions, i.e., $s_n^{\mathrm{ES}}(r) = s_{n-1}^{\mathrm{ES}}(r) - [r/(2n-1)][\partial s_{n-1}^{\mathrm{ES}}(r)/\partial r]$, as given below,

$$s_0^{\mathrm{ES}}(r) = \mathrm{erf}(\kappa_{\alpha\beta} r_{i_\alpha j_\beta}) - 0.5\,\mathrm{erf}(\kappa_{\alpha s} r_{i_\alpha j_\beta}) - 0.5\,\mathrm{erf}(\kappa_{\beta s} r_{i_\alpha j_\beta}) \tag{16}$$

$$s_1^{\mathrm{ES}}(r) = s_0^{\mathrm{ES}}(r) - (2r_{i_\alpha j_\beta}/\sqrt{\pi})[\kappa_{\alpha\beta}\exp(-\kappa_{\alpha\beta}{}^2 r_{i_\alpha j_\beta}{}^2) - 0.5\kappa_{\alpha s}\exp(-\kappa_{\alpha s}{}^2 r_{i_\alpha j_\beta}{}^2) - 0.5\kappa_{\beta s}\exp(-\kappa_{\beta s}{}^2 r_{i_\alpha j_\beta}{}^2)] \tag{17}$$

$$s_2^{\mathrm{ES}}(r) = s_1^{\mathrm{ES}}(r) - (4r_{i_\alpha j_\beta}{}^3/3\sqrt{\pi})[\kappa_{\alpha\beta}{}^3\exp(-\kappa_{\alpha\beta}{}^2 r_{i_\alpha j_\beta}{}^2) - 0.5\kappa_{\alpha s}{}^3\exp(-\kappa_{\alpha s}{}^2 r_{i_\alpha j_\beta}{}^2) - 0.5\kappa_{\beta s}{}^3\exp(-\kappa_{\beta s}{}^2 r_{i_\alpha j_\beta}{}^2)] \tag{18}$$

$$s_3^{\mathrm{ES}}(r) = s_2^{\mathrm{ES}}(r) - (8r_{i_\alpha j_\beta}{}^5/15\sqrt{\pi})[\kappa_{\alpha\beta}{}^5\exp(-\kappa_{\alpha\beta}{}^2 r_{i_\alpha j_\beta}{}^2) - 0.5\kappa_{\alpha s}{}^5\exp(-\kappa_{\alpha s}{}^2 r_{i_\alpha j_\beta}{}^2) - 0.5\kappa_{\beta s}{}^5\exp(-\kappa_{\beta s}{}^2 r_{i_\alpha j_\beta}{}^2)] \tag{19}$$

where $\kappa_{\alpha s} \equiv 1/[2(\sigma_\alpha{}^2 + \sigma_\beta{}^2)]^{1/2}$ and $\kappa_{\alpha\beta} = 1/[2(\sigma_\alpha{}^2 + \sigma_\beta{}^2)]^{1/2}$ resulting from the "Gaussian product rule" that describes the overlap of pairs of Gaussian distributions,[70,71] $\kappa_\alpha = (\sigma_\alpha\sqrt{2})^{-1}$, and $\kappa_s = (\sigma_s\sqrt{2})^{-1}$. Therefore, the Cartesian operators $\hat{T}(r) \equiv \mathrm{erf}(\kappa r)/r$, $\hat{T}^\gamma(r) \equiv \nabla_\gamma \hat{T}(r)$, and $\hat{T}^{\gamma\lambda}(r) \equiv \nabla_\lambda \hat{T}^\gamma(r)$ are formally the same as those given by eqs 11−13 except for the substitution of $s_n(r)$ by $s_n^{\mathrm{ES}}(r)$ as defined by eqs 16−19, where we included $s_3^{\mathrm{ES}}(r)$ because this one will be invoked later in the derivation of the corresponding force expressions. Note that, as we apply the limiting condition $\sigma_\alpha \to 0$ (i.e., $\kappa_\alpha \to \infty$), all these operators reduce to the corresponding expressions to point-charge and point-dipole distributions as described by Nymand et al.[72] after considering the missing minus signs in the second and fourth lines in their eq 2.

Now, the interaction energy given by eq 5—or corresponding expressions from the individual contributions, eqs 8−10—of an infinite periodically replicated system according to the Ewald summation approach involves four terms, i.e.,

$$U_{\mathrm{int}} = U_{\mathrm{real}}^{\mathrm{ES}} + U_{\mathrm{recp}}^{\mathrm{ES}} + U_{\mathrm{self\text{-}intra}}^{\mathrm{ES}} + U_{\mathrm{surf}}^{\mathrm{ES}} \tag{20}$$

where the real-space contributions become

$$U_{real}^{es} = \sum_{i=1}^{N}\sum_{\alpha=1}^{S_\alpha}\sum_{j>i}^{N}\sum_{\beta=1}^{S_\beta} \left[\underbrace{q_i^\alpha \hat{T}_{i_\alpha j_\beta} q_j^\beta}_{qq} + \underbrace{\mu_i^{ind,\gamma}\hat{T}_{ij_\beta}^\gamma q_j^\beta - q_i^\alpha \hat{T}_{i_\alpha j}^\gamma \mu_j^{ind,\gamma}}_{q\mu} - \underbrace{\mu_i^{ind,\gamma}\hat{T}_{ij}^{\gamma\lambda}\mu_j^{ind,\lambda}}_{\mu\mu} \right] \tag{21}$$

where S_α indicates the number of sites in the i molecule and

$$U_{\mathrm{real}-qq}^{\mathrm{ES}} = \sum_{i=1}^{N}\sum_{\alpha=1}^{S_\alpha}\sum_{j>i}^{N}\sum_{\beta=1}^{S_\beta} (q_i^\alpha q_j^\beta / r_{i_\alpha j_\beta})(\mathrm{erf}(\kappa_{\alpha\beta} r_{i_\alpha j_\beta}) - 0.5\,\mathrm{erf}(\kappa_{\alpha s} r_{i_\alpha j_\beta}) - 0.5\,\mathrm{erf}(\kappa_{\beta s} r_{i_\alpha j_\beta})) \tag{22}$$

$$U_{\mathrm{real}-q\mu}^{\mathrm{ES}} = -\sum_{i=1}^{N}\sum_{\alpha=1}^{S_\alpha}\sum_{j>i}^{N}\sum_{\beta=1}^{S_\beta} [\mu_i^{\mathrm{ind},\gamma} s_1^{\mathrm{ES}}(r)(r_{ij_\beta}^\gamma / r_{ij_\beta}{}^3) q_j^\beta - q_i^\alpha s_1^{\mathrm{ES}}(r)(r_{i_\alpha j}^\gamma / r_{i_\alpha j}{}^3)\mu_j^{\mathrm{ind},\gamma}] \tag{23}$$

$$U_{\mathrm{real}-\mu\mu}^{\mathrm{ES}} = -\sum_{i=1}^{N}\sum_{\alpha=1}^{S_\alpha}\sum_{j>i}^{N}\sum_{\beta=1}^{S_\beta} [\mu_i^{\mathrm{ind},\gamma}(s_2^{\mathrm{ES}}(r) 3 r_{ij}^\gamma r_{ij}^\lambda / r_{ij}{}^5 - s_1^{\mathrm{ES}}(r)\delta_{\gamma\lambda}/r_{ij}{}^3)\mu_j^{\mathrm{ind},\lambda}] \tag{24}$$

For the reciprocal space, after defining $\mathbf{h} = 2\pi(n_x/L_x, n_y/L_y, n_z/L_z)$, where $\mathbf{n} = (n_x, n_y, n_z)$ is a vector of integers and L_α is the side length of the unit cell, we introduce the structural factors for the electrostatic charges, $S^{qq}(h)$ and $T^{qq}(h)$, as well as for the induced dipoles, $S^{\mu\mu}(h)$ and $T^{\mu\mu}(h)$, defined as follows (see Appendix B in the Supporting Information for details)

$$S^{qq}(h) = \sum_{i=1}^{N}\sum_{\alpha=1}^{S_\alpha} q_i^\alpha \exp(i\mathbf{h}\cdot\mathbf{r}_{i_\alpha}) \tag{25}$$

$$T^{qq}(h) = \sum_{i=1}^{N}\sum_{\alpha=1}^{S_\alpha} q_i^\alpha \exp(-h^2/4\kappa_\alpha{}^2)\exp(i\mathbf{h}\cdot\mathbf{r}_{i_\alpha}) \tag{26}$$

$$S^{\mu\mu}(h) = \sum_{j=1}^{N} \boldsymbol{\mu}_j^{\mathrm{ind}}\cdot\nabla_j \exp(i\mathbf{h}\cdot\mathbf{r}_j) = \sum_{j=1}^{N} i(\boldsymbol{\mu}_j^{\mathrm{ind}}\cdot\mathbf{h})\exp(i\mathbf{h}\cdot\mathbf{r}_j) \tag{27}$$

$$T^{\mu\mu}(h) = \sum_{j=1}^{N} \boldsymbol{\mu}_j^{\mathrm{ind}}\cdot\nabla_j \exp(-h^2/4\kappa_\mu{}^2)\exp(i\mathbf{h}\cdot\mathbf{r}_j) = \sum_{j=1}^{N} i(\mu_j^{\mathrm{ind}}\cdot\mathbf{h})\exp(-h^2/4\kappa_\mu{}^2)\exp(i\mathbf{h}\cdot\mathbf{r}_j) \tag{28}$$

i.e., for the point-charge and Gaussian-charge density distributions, where $i = (-1)^{1/2}$. Moreover, following the ideas behind the derivation of the reciprocal-space contributions[47] after defining $S^{q\mu}(h) = S^{qq}(h) + S^{\mu\mu}(h)$, $T^{q\mu}(h) = T^{qq}(h) + T^{\mu\mu}(h)$, and $A(h) = \exp(-h^2/4\kappa_s{}^2)/h^2$, we have that

dx.doi.org/10.1021/jp509074p | J. Phys. Chem. B 2014, 118, 13658−13670

$$U^{ES}_{recp} = (\pi/V)\sum_{h\neq 0} A(h)[T^{q\mu}(h)S^{q\mu}(-h) + T^{q\mu}(-h)S^{q\mu}(h)] = (2\pi/V)\sum_{h\neq 0} A(h)\mathrm{Re}[T^{q\mu}(h)S^{q\mu}(-h)] \quad (29)$$

where Re indicates the real component of the complex quantity between brackets. Note that eq 29 reduces to eq A8 of Baranyai and Kiss,[32] or the alternative eq A1 of Jeon et al.,[73] in the absence of induced dipole moment, i.e., $S^{\mu\mu}(h) = T^{\mu\mu}(h) = 0$, as illustrated in Appendix B in the Supporting Information.

For the third term in eq 20, we apply the $r_{ij} \to 0$ limiting condition to eq 22 after invoking the power expansion for the operator $\hat{T}(r)$ and recalling that the unrestricted ij-summation is one-half of that for $j > i$ it follows that

$$\lim_{r_{ij}\to 0} \mathrm{erf}(\kappa_{\alpha s} r_{ij})/r_{ij} = \lim_{r_{ij}\to 0}(2\kappa_{\alpha s}/\sqrt{\pi} - 2\kappa_{\alpha s}{}^3 r_{ij}{}^2/3\sqrt{\pi} + O(r_{ij}{}^4)) = 2\kappa_{\alpha s}/\sqrt{\pi} \quad (30)$$

so that from eqs 22 and 30 we get the charge self and intramolecular interactions corrections that are formally the same as for point charges[72] but involving the parameters $\kappa_{\alpha s}$ and $\kappa_{\beta s}$ rather than κ_s, i.e.,

$$U^{es}_{self\text{-}intra} = \underbrace{\left[-\kappa_{\alpha s}/\sqrt{\pi}\right]\sum_{i=1}^{N}\sum_{\alpha=1}^{S_\alpha} q_i^\alpha q_i^\alpha}_{qq-self} - \underbrace{0.5\sum_{i=1}^{N}\sum_{\alpha<\beta=1}^{S_\alpha}\left(q_i^\alpha q_i^\beta/r_{i_\alpha i_\beta}\right)\left(erf(\kappa_{\alpha s} r_{i_\alpha i_\beta}) + erf(\kappa_{\beta s} r_{i_\alpha i_\beta})\right)}_{qq-intra} \quad (31)$$

Moreover, from eq 24, the induced dipole self-interactions can be calculated by recalling that

$$U^{ES}_{self-\mu\mu} = -0.5\lim_{\mu_i\to\mu_j}\sum_i (\boldsymbol{\mu}_i^{ind}\cdot\nabla_{ij})(\boldsymbol{\mu}_j^{ind}\cdot\nabla_{ji})\lim_{r_{ij}\to 0}(\mathrm{erf}(\kappa_{\mu s} r_{ij})/r_{ij}) \quad (32)$$

which, after invoking the power expansion in the right-hand side of eq 30 and the identity $\nabla_{ij} = -\nabla_{ji}$, we find that

$$\lim_{r_{ij}\to 0}\sum_i (\boldsymbol{\mu}_i^{ind}\cdot\nabla_{ij})(\boldsymbol{\mu}_j^{ind}\cdot\nabla_{ji})(2\kappa_{\mu s}/\sqrt{\pi} - 2\kappa_{\mu s}{}^3 r_{ij}{}^2/3\sqrt{\pi} + O(r_{ij}{}^4)) = (4\kappa_{\mu s}{}^3/3\sqrt{\pi})(\boldsymbol{\mu}_i^{ind}\cdot\boldsymbol{\mu}_i^{ind}) \quad (33)$$

and consequently

$$U^{ES}_{self-\mu\mu} = (-2\kappa_{\mu s}{}^3/3\sqrt{\pi})\sum_i (\boldsymbol{\mu}_i^{ind}\cdot\boldsymbol{\mu}_i^{ind}) \equiv -0.5\sum_i \boldsymbol{\mu}_i^{ind}\cdot\mathbf{E}_i^{\mu\mu-self} \quad (34)$$

As for the case of charge self-interactions, eq 34 applies only to systems involving finite κ_μ values; otherwise, a similar analysis to that for point charges leads to $U^{ES}_{self-\mu\mu} = -(2\kappa_s{}^3/3\sqrt{\pi})\sum_i(\mu_i^{ind}\cdot\mu_i^{ind})$, i.e., $\kappa_s = \lim_{\kappa_\mu\to\infty}\kappa_{\mu s}$, for the case of induced point-dipoles as given by eqs 53−56 in ref 74.

Finally, the last term in eq 20 corresponds to the $\mathbf{h} = 0$ term in the Ewald summation and is given by[44]

$$U^{ES}_{surf} = (2\pi/(2\varepsilon_{RF}+1)V)[\sum_i (\boldsymbol{\mu}_i^{ind} + \sum_\alpha q_i^\alpha \mathbf{r}_{i_\alpha})]^2 \quad (35)$$

where $(\boldsymbol{\mu}_i^{ind} + \sum_\alpha q_i^\alpha \mathbf{r}_{i_\alpha})$ is the total dipole moment of molecule i and ε_{RF} is the dielectric permittivity accounting for the surroundings of the infinitely replicated system.

In order to assess all four contributions, we need first to minimize $U_{el}(\{\boldsymbol{\mu}_i^{ind}\})$, i.e., by solving the implicit equation $\boldsymbol{\mu}_i^{ind} = \alpha_i[\mathbf{E}_i^{qq} + \mathbf{E}_i^{\mu\mu}(\{\boldsymbol{\mu}_i^{ind}\})]$, and for that we must derive the corresponding Ewald expressions for the electric field components. Following a similar partition as for eq 20, we express the Cartesian component γ of the total electric field at the center of mass of molecule i in terms of the four Ewald contributions, i.e.,

$$E_{i,\gamma} = E^{real}_{i,\gamma} + E^{recp}_{i,\gamma} + E^{self\text{-}intra}_{i,\gamma} + E^{surf}_{i,\gamma} \quad (36)$$

For that purpose, we start by determining the electrostatic fields and their gradients from U_{el} according to the method proposed recently by Stenhammar et al.[75] to deal properly with periodic systems. After adding an infinitesimal Gaussian charge $\delta q(r)$ characterized by the exponent κ_δ we have that the electric potential $\phi(r) = \lim_{\delta q\to 0}(\partial U^{N+1}_{int}/\partial\delta q)$, the real-space contribution to the γ-component of the electric field becomes $E_\gamma(\mathbf{r}_i) = -\lim_{\mathbf{r}\to\mathbf{r}_i}(\partial\phi(\mathbf{r})/\partial r_\gamma)$, and the β-component of its gradient reads $E_{\lambda\beta}(\mathbf{r}_i) = -\lim_{\mathbf{r}\to\mathbf{r}_i}(\partial^2\phi(\mathbf{r})/\partial r_\gamma\partial r_\beta)$, i.e.,

$$E^{real}_{i,\gamma} = \sum_{j\neq i=1}^{N}\sum_{\beta=1}^{S_\beta}(-\hat{T}^\gamma_{ij_\beta}(r_{ij_\beta})q_j^\beta + \hat{T}^{\gamma\lambda}_{ij}(r_{ij})\mu_j^{ind,\lambda}) = \sum_{j\neq i=1}^{N}\sum_{\beta=1}^{S_\beta}(s_1^{ES}(r_{ij_\beta})q_j^\beta r^\gamma_{ij_\beta}/r_{ij_\beta}{}^3 + [s_2^{ES}(r_{ij})3r^\gamma_{ij}r^\lambda_{ij}/r_{ij}{}^5 - s_1^{ES}(r_{ij})\delta_{\gamma\lambda}/r_{ij}{}^3]\mu_j^{ind,\lambda}) \quad (37)$$

where the prefactors $s_l(r)$ are given by eqs 16−19.

For the reciprocal-space contribution to the electrostatic potential, and according to eq 29, we need to determine $\lim_{\delta q\to 0}(\partial S^{q\mu}_{N+1}/\partial\delta q)$ and $\lim_{\delta q\to 0}(\partial T^{q\mu}_{N+1}/\partial\delta q)$, i.e.,

$$\phi^{ES}_{recp}(r) = (\pi/V)\sum_{h\neq 0} A(h)\{[T^{q\mu}(h)(\partial S^{q\mu}(-h)/\partial\delta q)_{\delta q\to 0} + S^{q\mu}(-h)(\partial T^{q\mu}(h)/\partial\delta q)_{\delta q\to 0} + T^{q\mu}(-h)(\partial S^{q\mu}(h)/\partial\delta q)_{\delta q\to 0} + S^{q\mu}(h)(\partial T^{q\mu}(-h)/\partial\delta q)_{\delta q\to 0}]\} = (2\pi/V)\sum_{h\neq 0} A(h)\mathrm{Re}\{[T^{q\mu}(h) + S^{q\mu}(h)\exp(-h^2/4\kappa_\alpha{}^2)]\times\exp(-i\mathbf{h}\cdot\mathbf{r})\} \quad (38)$$

so that the γ-component of the field gradient becomes

dx.doi.org/10.1021/jp509074p | J. Phys. Chem. B 2014, 118, 13658−13670

$$E_{i,\gamma}^{\mathrm{recp}}(r_i) = -\lim_{\mathbf{r}\to\mathbf{r}_i}(\partial\phi(\mathbf{r})/\partial r_\gamma)$$
$$= -\lim_{\mathbf{r}\to\mathbf{r}_i}(2\pi/V) \sum_{h\neq 0} A(h)\{\mathrm{Re}[-ih_\gamma T^{q\mu}(h)\exp(-i\mathbf{h}\cdot\mathbf{r}) + ih_\gamma S^{q\mu}(-h)\exp(i\mathbf{h}\cdot\mathbf{r})\exp(-h^2/4{\kappa_\alpha}^2)]\}$$
$$= -(2\pi/V)\sum_{h\neq 0} A(h)h_\gamma \mathrm{Im}\{[T^{q\mu}(h) + S^{q\mu}(h)\exp(-h^2/4{\kappa_\alpha}^2)] \times \exp(-i\mathbf{h}\cdot\mathbf{r}_i)\} \quad (39)$$

where Im denotes the imaginary part of the complex quantity between curly brackets. Likewise, the corresponding intramolecular interaction energy expression becomes

$$E_{i,\gamma}^{\mathrm{intra}} = \sum_{i=1}^{N}\sum_{\alpha\neq\beta=1}^{S_\alpha} \hat{T}^{\gamma}_{i_\alpha i_\beta}(r_{i_\alpha i_\beta}) q_i^\beta = -\sum_{i=1}^{N}\sum_{\alpha\neq\beta=1}^{S_\alpha} s_1^{\mathrm{ES}}(r_{i_\alpha i_\beta}) q_i^\beta r_{i_\alpha i_\beta}^\gamma / {r_{i_\alpha i_\beta}}^3 \quad (40)$$

i.e., there is not a contribution from the induced dipole, since the i_α is the center-of-mass site where the induced dipole is also located. Moreover, the induced dipole self-contributions follow from eq 34, i.e.,

$$E_{i,\gamma}^{\mu\mu-\mathrm{self}} = (4{\kappa_{\mu s}}^3/3\sqrt{\pi})\mu_i^{\mathrm{ind},\gamma} \quad (41)$$

Finally, according to eq 35, the surface contribution corresponding to $\mathbf{h} = 0$ becomes

$$E_{i,\gamma}^{\mathrm{surf}} = -(4\pi/(2\varepsilon_{\mathrm{RF}}+1)V)\sum_j (\mu_j^{\mathrm{ind},\gamma} + \sum_\beta q_j^\beta r_{j_\beta}^\gamma) \quad (42)$$

This completes the derivation of the expressions needed for the self-consistent calculation of the induced dipole moments, i.e., the solution of the implicit eq 15 when the electrostatic interactions of the GCP model are described by an Ewald summation approach.

b. Force Calculation. According to eq 20 and its four contributions, after invoking the definition for the λ-Cartesian component of the force in the α-site of the i-molecule, i.e., $f_{i_\alpha}^\lambda(r_{i_\alpha}) = -\nabla_\lambda U(r_{i_\alpha})$, we have that

$$f_{i_\alpha}(r_{i_\alpha})_\lambda = f_{i_\alpha}^{\mathrm{real}}(r_{i_\alpha})_\lambda + f_{i_\alpha}^{\mathrm{recp}}(r_{i_\alpha})_\lambda + f_{i_\alpha}^{\text{self-intra}}(r_{i_\alpha})_\lambda + f_{i_\alpha}^{\mathrm{surf}}(r_{i_\alpha})_\lambda \quad (43)$$

where

$$f_{i_\alpha}^{real}(r_{i_\alpha})_\lambda = -\sum_{j>i}^{N}\sum_{\beta=1}^{S_\beta} \left[\underbrace{q_i^\alpha \hat{T}^\lambda_{i_\alpha j_\beta} q_j^\beta}_{qq} + \underbrace{\mu_i^{ind\gamma}\hat{T}^{\gamma\lambda}_{ij_\beta} q_j^\beta - q_i^\alpha \hat{T}^{\gamma\lambda}_{i_\alpha j}\mu_j^{ind,\gamma}}_{q\mu} - \underbrace{\mu_i^{ind\gamma}\hat{T}^{\gamma\delta\lambda}_{ij}\mu_j^{ind,\delta}}_{\mu\mu}\right] \quad (44)$$

with the operators $\hat{T}^\lambda_{i_\alpha j_\beta}(r)$ and $\hat{T}^{\gamma\lambda}_{ij_\beta}(r)$ formally the same as those in eqs 12 and 13, while $\hat{T}^{\gamma\delta\lambda}_{ij}(r)$ is given by

$$\hat{T}_{ij}^{\gamma\delta\lambda}(r) \equiv \nabla_\gamma \hat{T}_{ij}^{\delta\lambda}(r) = -15 s_3^{\mathrm{ES}} r_{ij}^\gamma r_{ij}^\delta r_{ij}^\lambda / {r_{ij}}^7 + 3 s_2^{\mathrm{ES}}(r)[\delta_{\gamma\delta} r_{ij}^\lambda + \delta_{\delta\lambda} r_{ij}^\gamma + \delta_{\lambda\gamma} r_{ij}^\delta]/{r_{ij}}^5 \quad (45)$$

and the prefactors $s_2^{\mathrm{ES}}(r)$ and $s_3^{\mathrm{ES}}(r)$ are given by eqs 18 and 19. Likewise, from eq 29, after recalling that the induced dipole sits on the center of mass, we have that

$$f_{i_\alpha}^{\mathrm{recp}}(r_{i_\alpha})_\lambda = -(2\pi/V)\sum_{h\neq 0} A(h)h_\lambda q_i^\alpha \times \mathrm{Im}\{[S^{q\mu}(h)\exp(-h^2/4{\kappa_\alpha}^2) + T^{q\mu}(h)] \exp(-i\mathbf{h}\cdot\mathbf{r}_{i_\alpha})\} \quad (46)$$

for the charged sites and

$$f_{i_\alpha}^{\mathrm{recp}}(r_{i_\alpha})_\lambda = -(2\pi/V)\sum_{h\neq 0} A(h)h_\lambda \delta_{i_\alpha i}(\boldsymbol{\mu}_i^{\mathrm{ind}}\cdot\mathbf{h}) \times \mathrm{Im}\{[S^{q\mu}(h)\exp(-h^2/4{\kappa_\mu}^2) + T^{q\mu}(h)] \exp(-i\mathbf{h}\cdot\mathbf{r}_i)\} \quad (47)$$

for the molecular center-of-mass site. Note that in the absence of induced dipole moments eq 47 reduces to eq A9 of Baranyai and Kiss.[32]

Now, if we invoke the limiting $\kappa_\mu, \kappa_\alpha \to \infty$ condition for eqs 46 and 47, respectively, the above expressions become those of Nymand et al.[72]

$$f_{i_\alpha}^{\mathrm{recp}}(r_{i_\alpha}, \kappa_\alpha\to\infty)_\lambda = -(4\pi/V)\sum_{h\neq 0} A(h)h_\lambda q_i^\alpha \mathrm{Im}\{Q^{q\mu}(h)\exp(-i\mathbf{h}\cdot\mathbf{r}_{i_\alpha})\} \quad (48)$$

for the charge sites of the molecule comprising point charges and induced point dipoles while

$$f_{i_\alpha}^{\mathrm{recp}}(r_{i_\alpha}, \kappa_\mu\to\infty)_\lambda = (4\pi/V)\sum_{h\neq 0} A(h)h_\lambda \delta_{i_\alpha i}(\boldsymbol{\mu}_i^{\mathrm{ind}}\cdot\mathbf{h})\,\mathrm{Im}\{Q^{q\mu}(-h) \exp(i\mathbf{h}\cdot\mathbf{r}_i)\} \quad (49)$$

provides the force at the corresponding center-of-mass induced point-dipole site, after invoking the identity $\mathrm{Im}\{Q^{q\mu}(h)\exp(-i\mathbf{h}\cdot\mathbf{r}_i)\} = -\mathrm{Im}\{Q^{q\mu}(-h)\exp(i\mathbf{h}\cdot\mathbf{r}_i)\}$.

Moreover, the self-intra contributions are formally the same as per eq 44, i.e.,

$$f_{i_\alpha}^{self-intra}(r_{i_\alpha})_\lambda = \sum_{\beta>\alpha=1\in i}^{S_\beta} \left[\underbrace{q_i^\alpha \hat{T}^\lambda_{i_\alpha i_\beta} q_i^\beta}_{qq} + \underbrace{\mu_{i_\alpha}^{ind,\gamma}\hat{T}^{\gamma\lambda}_{i_\alpha i_\beta} q_i^\beta - \overbrace{q_i^\alpha \hat{T}^{\gamma\lambda}_{i_\alpha i_\beta}\mu_{i_\beta}^{ind,\gamma}}^{\beta>\alpha=1\therefore 0}}_{q\mu} - \underbrace{\overbrace{\mu_{i_\alpha}^{ind,\gamma}\hat{T}^{\gamma\delta\lambda}_{i_\alpha i_\beta}\mu_{i_\beta}^{ind,\delta}}^{\beta>\alpha=1\therefore 0}}_{\mu\mu}\right] \quad (50)$$

where $\beta > \alpha = 1 \in i$ highlights the fact that sites α and β belong to the same i-molecule; consequently, the corresponding last two terms in eq 50 do not contribute to $f_{i_\alpha}^{\text{self-intra}}(r_{i_\alpha})_\lambda$. Finally, from eq 35, the force expression for the surface correction becomes

dx.doi.org/10.1021/jp509074p | J. Phys. Chem. B 2014, 118, 13658−13670

$$f_{i_\alpha}^{\mathrm{surf}}(r_{i_\alpha})_\lambda = -(4\pi/(2\varepsilon_{\mathrm{RF}}+1)V)\Big(\sum_j \boldsymbol{\mu}_j^{\mathrm{ind}} + \sum_{j_\beta} q_j^\beta \mathbf{r}_{j_\beta}\Big)_\lambda q_i^\alpha \tag{51}$$

c. Virial Calculation. After having derived the electrostatic energy and force expressions, we need to obtain the corresponding virial Φ starting from its definition[76]

$$\Phi = 3V\langle \partial U(V)/\partial V\rangle \tag{52}$$

where $\langle\cdots\rangle$ denotes an ensemble average, with $U = U_{\mathrm{disp}} + U_{\mathrm{el}}$ from eqs 1 and 4, we have that the total pressure $p = NkT/V - \Phi/3V$. Now, by invoking the scaling of particle positions with the cell dimension,[77] i.e., $\mathbf{r}_{i_\alpha j_\beta} = V^{1/3}\boldsymbol{\rho}_{ij} + \mathbf{d}_{i_\alpha} - \mathbf{d}_{i_\beta}$, where $V^{1/3}\boldsymbol{\rho}_i = \mathbf{r}_i$ denotes the center of mass of particle i, and consequently $\mathbf{r}_{i_\alpha} = \mathbf{r}_i + \mathbf{d}_{i_\alpha}$ is the vector location of its site α, we have that $\partial_{i_\alpha j_\beta}/\partial V = \mathbf{r}_{i_\alpha j_\beta}\cdot\mathbf{r}_{ij}/(3Vr_{i_\alpha j_\beta})$. Therefore, from eq 52, we can express the total virial associated with the electrostatic interactions as follows

$$\begin{aligned}\Phi_{\mathrm{int}} &= 0.5\Big\langle \sum_{j\neq i}\sum_{\alpha,\beta} (\partial u(r_{i_\alpha j_\beta})/\partial r_{i_\alpha j_\beta})\hat{\mathbf{r}}_{i_\alpha j_\beta}\cdot\mathbf{r}_{ij}\Big\rangle \\ &= -\Big\langle 0.5\sum_{j\neq i}\sum_{\alpha,\beta}\mathbf{f}_{i_\alpha j_\beta}\cdot\mathbf{r}_{i_\alpha j_\beta} - \sum_i\sum_\alpha \mathbf{f}_{i_\alpha}\cdot\mathbf{d}_{i_\alpha}\Big\rangle\end{aligned} \tag{53}$$

where we should recall that, according to eq 20, we need to determine explicitly the four individual contributions, i.e.,

$$\Phi_{\mathrm{int}} = \Phi_{\mathrm{real}}^{\mathrm{ES}} + \Phi_{\mathrm{recp}}^{\mathrm{ES}} + \Phi_{\mathrm{self\text{-}intra}}^{\mathrm{ES}} + \Phi_{\mathrm{surf}}^{\mathrm{ES}} \tag{54}$$

Below we quote the final expression for Φ_{int} whose explicit derivation is given in Appendix C in the Supporting Information, i.e.,

$$\begin{aligned}\Phi = &-\Big\langle 0.5\sum_{j\neq i}\sum_{\alpha,\beta}\mathbf{f}_{i_\alpha j_\beta}^{\mathrm{real}}\cdot\mathbf{r}_{i_\alpha j_\beta}\Big\rangle + \Big\langle\sum_i\sum_\alpha(\mathbf{f}_{i_\alpha}^{\mathrm{real}} + \mathbf{f}_{i_\alpha}^{\mathrm{recp}} + \mathbf{f}_{i_\alpha}^{\mathrm{surf}})\cdot\mathbf{d}_{i_\alpha}\Big\rangle \\ &- \langle 2\pi/V\sum_{h\neq 0} A(h)[1 - (h^2/2\kappa_s^2)]\ \mathrm{Re}[T^{q\mu}(h)S^{q\mu}(-h)]\rangle \\ &- \langle 2\pi/V\sum_{h\neq 0} A(h)\ \mathrm{Re}[T^{\mu\mu}(h)S^{q\mu}(-h) + T^{q\mu}(h)S^{\mu\mu}(-h)]\rangle \\ &+ \langle 2\pi/V\sum_{h\neq 0} A(h)\ \mathrm{Re}[\{\sum_{i=1}^{N}\sum_{\alpha=1}^{S_\alpha} q_i^\alpha(h^2/2\kappa_\alpha^2)\exp(-h^2/4\kappa_\alpha^2)\exp(i\mathbf{h}\cdot\mathbf{r}_{i_\alpha}) \\ &+ \sum_{j=1}^{N} i(\boldsymbol{\mu}_j^{\mathrm{ind}}\cdot\mathbf{h})(h^2/2\kappa_\mu^2)\exp(-h^2/4\kappa_\mu^2)\exp(i\mathbf{h}\cdot\mathbf{r}_j)\}S^{q\mu}(-h)]\rangle \\ &- \langle(U_{\mathrm{surf}}^{qq,\mathrm{ES}} + 2U_{\mathrm{surf}}^{q\mu,\mathrm{ES}} + 3U_{\mathrm{surf}}^{\mu\mu,\mathrm{ES}})\rangle\end{aligned} \tag{55}$$

IV. SIMULATION DETAILS AND RESULTS

The main thrust behind these simulations is to compare the outcome from the derived Ewald formalism against the corresponding RF approach, illustrate the thermodynamic and microstructural behavior of water at three contrasting extreme local environments, and simultaneously provide some relevant details underlying the simulation implementation of the Ewald summation for this type of electrostatic model. All simulations were performed at isobaric−isothermal conditions, in a cubic cell of dimension L involving either $N = 256$ molecules at the state conditions indicated in Table 1, where the isothermal conditions were achieved through independent Nosé thermostats for the rotational and translational degrees of freedom[78,79] and the isobaric conditions were controlled by Nosé−Andersen's barostat.[77,79] These conditions were chosen because (a) they represent contrasting hydrogen-bonded environments of geological interest characterized by significantly different nearest-neighbor environments, (b) there are experimental data available for their microstructure from neutron scattering with isotopic substitution and X-ray diffraction, and consequently (c) they become a suitable target to investigate the poorly understood or currently unknown spatial distribution functions for some relevant microstructural quantities.

Table 1. Water State Conditions and References for the Microstructural Data

system	T (K)	ρ (g/cc)	p (GPa)	ref
1	298	0.997	0.0001	80
2	673	0.872	0.34	80
3	500	1.437[a]	4.1	81

[a]Estimated according to Sanchez-Valle et al.'s equation of state.[82]

The integration of the molecular Newton−Euler equations of motion were done through fourth-order Gear's predictor-corrector algorithms for the translational degrees of freedom (second order ODE), and the rotational degrees of freedom (first order ODE)[83] based on the Evans−Murad quaternion formalism[84] involving a time-step size of 1.0 fs. After an equilibration period of 50 ps, all simulations were run for about 0.5 ns during which all average quantities were computed and their uncertainties were determined following the block-average approach proposed by Flyvbjerg and Petersen.[85] All interactions were truncated at a cutoff radius $r_c = 0.5L$, under standard 3D periodic boundary conditions so that each molecule interacts with the nearest image of all the other molecules, where the van der Waals configurational properties were corrected by the corresponding long-range contributions assuming uniform density distributions for distances $r > r_c$ (see Appendix D in the Supporting Information for details).

We originally applied the first-order predictor-iterative method proposed by Ahlström et al.[61] to solve self-consistently the implicit eq 15. This method utilizes the induced dipole moments of the previous two time steps as initial conditions for the predictor-iterative process, and typically requires five iterations to achieve dipole convergence within an absolute error given by $\max(\mu_i^{\mathrm{ind(new)}} - \mu_i^{\mathrm{ind(old)}}) \leq 5\times 10^{-5}$ D[31] within the context of a reaction-field approach for the electrostatic interactions. In the present case, we implemented Kolafa's Always Stable Predictor-Corrector (ASPC) method[86] that avoids the need for the iteration step, and consequently reduces significantly the computational cost of the induced dipole calculations. In particular, we chose the $k = 2$ version of ASPC where the first step predicts the new sets of induced dipole moments $\{\boldsymbol{\mu}_i^{\mathrm{ind\text{-}pred}}(t+\Delta t)\}$ is predicted in terms of the $k + 2$ previous time steps, i.e.,

$$\{\boldsymbol{\mu}_i^{\mathrm{ind-pred}}(t+\Delta t)\} = \sum_{l=0}^{k+1} B_{l+1}\{\boldsymbol{\mu}_i^{\mathrm{ind}}(t - l\Delta t)\} \tag{56}$$

where the $B_l(k)$ are given in Table 1 of ref 86. These predicted values are then corrected according to the following expression

$$\begin{aligned}\{\boldsymbol{\mu}_i^{\mathrm{ind}}(t+\Delta t)\} = \omega[\alpha_i(\mathbf{E}_i^{qq} + \mathbf{E}_i^{\mu\mu}\{\boldsymbol{\mu}_i^{\mathrm{ind-pred}}(t+\Delta t)\})] \\ + (1-\omega)\{\boldsymbol{\mu}_i^{\mathrm{ind-pred}}(t+\Delta t)\}\end{aligned} \tag{57}$$

where the relaxation parameter ω is chosen (ω greater than or approximately equal to 4/7 in our case) to ensure the stability of the calculations.

For the implementation of the Ewald summation, we chose $\kappa_s = (\sigma_s\sqrt{2})^{-1}$ to ensure the proper convergence of the

dx.doi.org/10.1021/jp509074p | J. Phys. Chem. B 2014, 118, 13658−13670

electrostatic energy to achieve the desired accuracy at the lowest computational cost. For that purpose, we ran a series of one-step simulations over a wide range of κ_s along representative values of h_{max} and searched for the region of convergence of the electrostatic energy, as illustrated in Figure 2 for an infinitely replicated system surrounded by a continuum

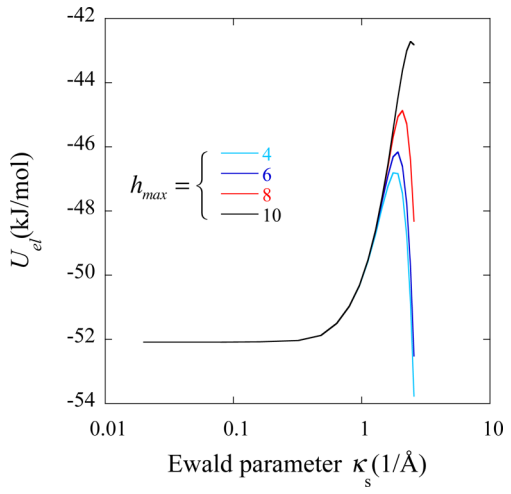

Figure 2. Electrostatic potential energy as a function of the Ewald attenuation parameter and parametric to the representative values of reciprocal-space cutoff.

dielectric with a permittivity of $\varepsilon_{RF} \approx 78$ under ambient conditions. According to Figure 2, and for all practical purposes, an adequate convergence occurs for $\kappa_s < 0.25$ Å^{-1} where the electrostatic energy becomes independent of h_{max}, suggesting that for the system size under consideration, e.g., real-space cutoff $r_c \cong 9.5$ Å, the largest contribution to the electrostatic energy comes from the real-space contributions to the Ewald summation.

Here we present a comparison between the properties of the GCP model of water according to the reaction field and the proposed Ewald summation implementation to account for the long-ranged electrostatic interactions. To assess the equivalence of the outcome between the two approaches, we studied the microstructural behavior of water in terms of the conventional radial distribution functions, $g_{OO}(r)$, $g_{OH}(r)$, and $g_{HH}(r)$ for the O···O, O···H, and H···H pair interactions, respectively. Among several relevant descriptors of the polarizable behavior of the GCP model,[58] we determined the magnitude of the average induced and total dipole moments as well as their relative orientation, in addition to the configurational energy (and its three relevant contributions) and the average density at the prescribed temperature and pressure as collected in Tables 2 and 3.

These tables clearly indicate the significant agreement between the proposed Ewald treatment and the current RF approach to the electrostatics of the GCP Hamiltonian.

In Figures 3−5, we display the standard orientational-averaged radial distribution functions for the three state conditions, where this comparison indicates that the reaction-field and Ewald summation implementations of the GCP model provide essentially identical microstructures. Moreover, in Figures 6−8, we display the comparison between the GCP water simulated structure and the corresponding available data from neutron diffraction with isotopic substitution (NDIS)[80] and X-ray diffraction experiments.[81,87] Although we have previously illustrated the agreement between simulation and NDIS under ambient conditions (e.g., Figure 5 of ref 31), here we add the comparison between simulation and the latest X-ray diffraction data for $g_{OO}(r)$ in Figure 6. The GCP model captures properly the significant structure changes undergone by water under extreme conditions of temperature and pressure. In particular, we note the increase in the O···O coordination from the original value of ∼4.4 under ambient conditions, to ∼10.3 at T = 673 K and p = 0.34 GPa, and to ∼13.3 at T = 500 K and p = 4.1 GPa.

In addition, note the noticeable right shift in the location of the first two peaks of $g_{OO}(r)$ at T = 673 K and p = 0.34 GPa (Figure 7) with respect to that of water at ambient conditions that translates into an increase in the water coordination by ∼6 additional water molecules from the original tetrahedral four-coordinated nearest-neighbor structure. This shift represents a drastic distortion of the original tetrahedral configurations of ambient water characterized by the first two $g_{OO}(r)$ peaks located at $r \simeq 2.78$ Å, $r \simeq 4.4$ Å, and clearly manifested/captured by the corresponding decrease of the tetrahedrality parameter from $q_T^{bulk} \simeq 0.63$ to $q_T^{bulk} \simeq 0.43$. Likewise, in Figure 8, we plot the $g_{OO}(r)$ of water at T = 500 K and p = 4.1 GPa as described by the GPC water model in comparison with the corresponding structural information for the O···O distribution from X-ray diffraction,[81] where we observe the significant increase in the population of the first and second nearest-neighbors, with respect to that at T = 673 K and p = 0.34 GPa, translating into a very closed packing of ∼13 water molecules in the first coordination shell and $q_T^{bulk} \simeq 0.49$.

Table 2. Comparison of Relevant Average Quantities from NPT-MD Simulations of the GCP Model Using the Reaction-Field (RF) and Ewald Summation (ES) Implementations

	system					
	1		2		3	
approach	RF	ES	RF	ES	RF	ES
T (K)	298	298	673	673	500	500
ρ (g/cc)	0.999(8)	1.007(8)	0.846(3)	0.854(3)	1.403(1)	1.410(1)[c]
φ^a (deg)	17.0(5)	17.0(5)	28.0(5)	28.0(5)	19.0(5)	19.0(5)
$\langle\mu_{tot}\rangle$ (D)	2.71(1)	2.71(1)	2.40(1)	2.40(1)	2.74(1)	2.73(1)
$\langle\mu^{ind}\rangle$ (D)	0.89(1)	0.89(1)	0.60(1)	0.60(1)	0.92(1)	0.91(1)
U_c^b	−44.2(1)	−44.3(1)	−27.6(1)	−27.7(1)	−35.6(1)	−35.5(1)

[a]Angle between the induced and permanent dipole moments of water. [b]In units of kJ/mol. [c]1.410(1) means 1.410 ± 0.001.

dx.doi.org/10.1021/jp509074p | J. Phys. Chem. B 2014, 118, 13658−13670

Table 3. Comparison of the Resulting Partial Contributions to the Total Configurational Energy (in kJ/mol) of the GCP model Using the Reaction-Field (RF) and Ewald Summation (ES) Implementations

	system					
	1		2		3	
approach	RF	ES	RF	ES	RF	ES
T (K)	298	298	673	673	500	500
U_{m_exp6}	9.2(1)[a]	9.3(1)	4.5(1)	4.6(1)	19.3(1)	19.4(1)
U_{qq}	−40.3(1)	−40.4(1)	−25.2(1)	−25.3(1)	−40.4(1)	−40.5(1)
U_{ind}	−13.0(1)	−12.9(1)	−6.8(1)	−6.7(1)	−14.2(1)	−13.9(1)

[a] 9.2(1) means 9.2 ± 0.1.

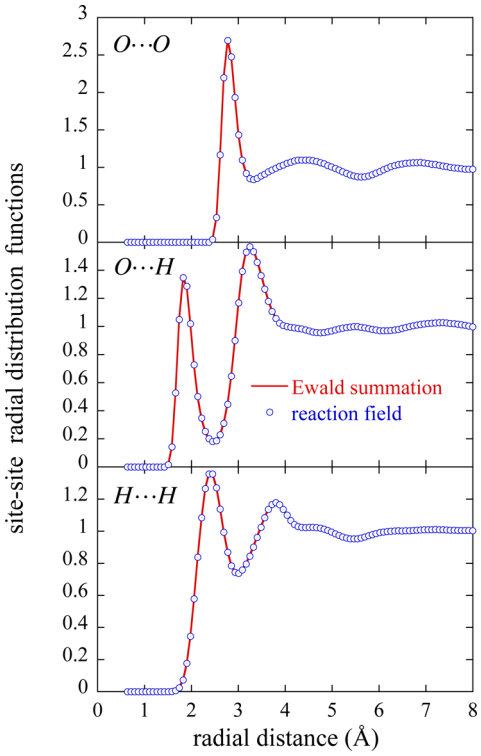

Figure 3. Comparison between the Ewald summation and the reaction-field outcomes for the site−site pair distribution functions of the GCP water at T = 298 K and p = 0.0001 GPa.

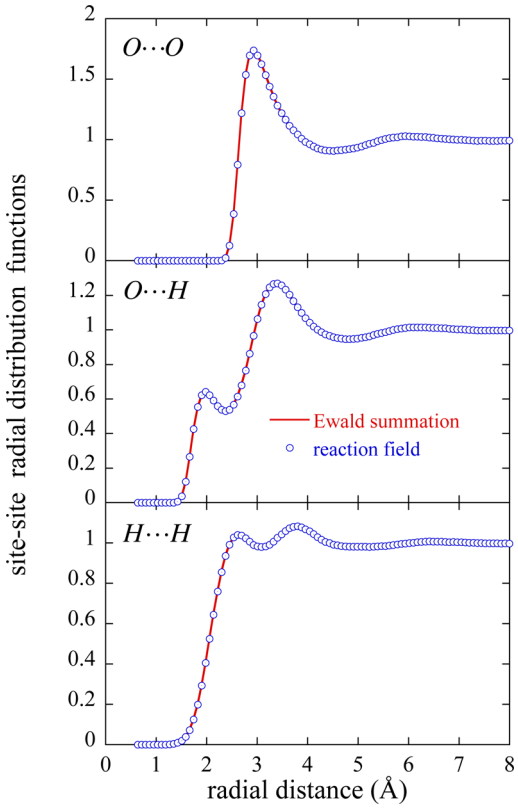

Figure 4. Comparison between the Ewald summation and the reaction-field outcomes for the site−site pair distribution functions of the GCP water at T = 673 K and p = 0.34 GPa.

V. DISCUSSION AND FINAL REMARKS

The proper treatment of long-ranged electrostatic interactions in systems under periodic boundary conditions involving polarizable species (including neutral molecules and ions) is a crucial requirement for the accurate description of the solvation properties of polar fluids and resulting electrolyte solutions,[40,88−90] and typically involves the implementation of rather contrasting methodologies, e.g., either a reaction-field or an Ewald summation approach. Because these two approaches are obviously not formally equivalent—the reaction field invokes the truncation of electrostatic interactions at a finite distance and corrects them for the long-ranged missing contributions, while the Ewald summation treats the system as a truly periodic infinitely replicated lattice—in principle, we should expect some differences in the simulated equilibrium thermodynamic and structural as well as dynamical quantities.[91]

Our NPT-MD simulation results for the microstructure, polarization, and thermodynamic behavior of bulk water under contrasting state conditions indicate a remarkable agreement between the original reaction field and the currently proposed Ewald summation implementation, where the agreement does not appear to be the consequence of cancellation of uncertainties among the different contributions to the electrostatic energy but a measure of the numerical equivalence between the two implementations. From a purely physical point of view, these results illustrate the microscopic complexity underlying the hydrogen-bonded water network, and the inability of nonpolarizable water models to describe the spatial inhomogeneous polarization distribution, with far reaching consequences in the description of hydration phenomena involving polar and ionic species.[92]

The developments in section II (e.g., eqs 5−10 and corresponding appendices A and B in the Supporting Information) provide the means to clarify some theoretical issues underlying the GCP modeling and the conceptual differences with the recently introduced Gaussian damping function technique to overcome overpolarization.[16,34,93] On the

dx.doi.org/10.1021/jp509074p | J. Phys. Chem. B 2014, 118, 13658−13670

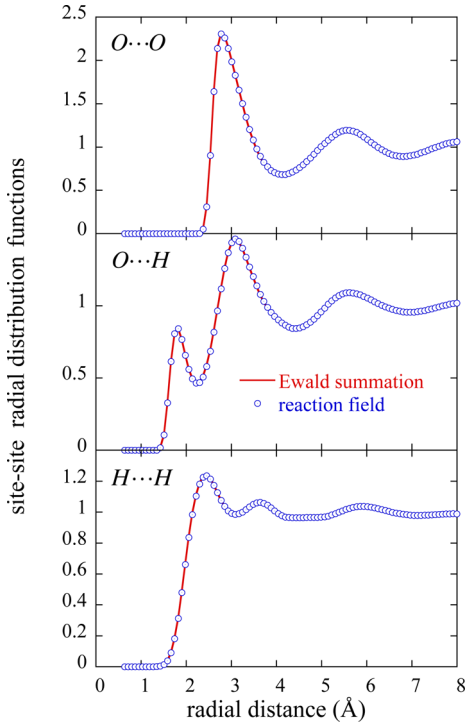

Figure 5. Comparison between the Ewald summation and the reaction-field outcomes for the site−site pair distribution functions of the GCP water at T = 500 K and p = 4.1 GPa.

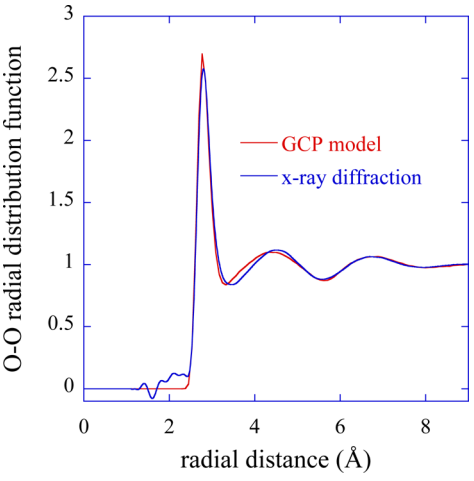

Figure 6. Comparison between the simulation results and X-ray diffraction data[86] for the O···O pair distribution functions of the GCP water at T = 298 K and p = 0.0001 GPa.

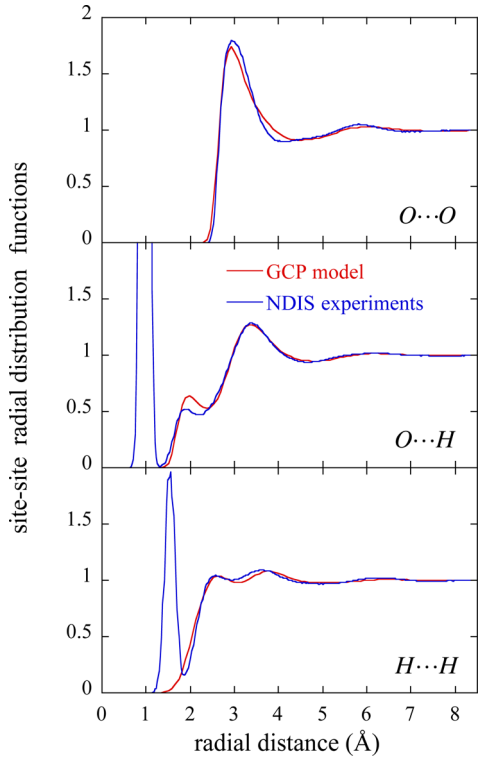

Figure 7. Comparison between the simulation results and neutron diffraction with isotopic substitution experimental data[80] for the site−site pair distribution functions of the GCP water at T = 673 K and p = 0.34 GPa.

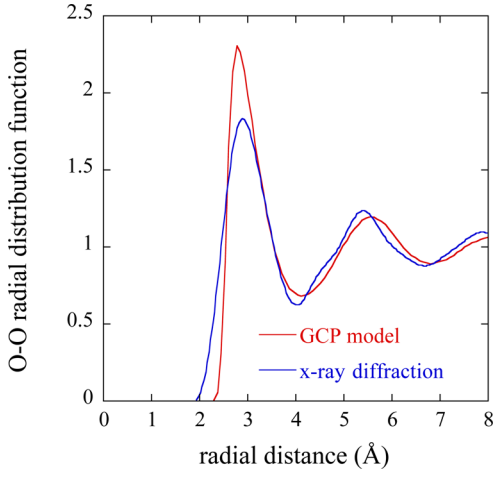

Figure 8. Comparison between the simulation results and X-ray diffraction data[81] for the O···O pair distribution functions of the GCP water at T = 500 K and p = 4.1 GPa.

one hand, the authors of ref 32 in their modeling discussion wrongly stated that "the disadvantage of the GCP model, however, is the use of a point dipole", since the actual GCP Hamiltonian involves Gaussian (i.e., given by eq 7) rather than point induced dipoles. On the other hand, in their discussion regarding the use of Gaussian damping of point-based electrostatics, the authors of ref 93 indicated that "In passing, we should also mention that some authors have used Gaussian charge polarizable models for simulating water.[47−49] According to the above discussion, those models are formally equivalent to point charge models with intermolecular Gaussian damping" (where 47−49 refers to citations in ref 93 and ref 47 identifies the GCP model). While the use of Gaussian damping functions in point-based electrostatic models might target the same overpolarization phenomenon as per the GCP model, a careful inspection of the underlying ideas and resulting expressions of the full electrostatic Hamiltonian for the GCP water does not support the idea of a "formal equivalence" as suggested in the above quote from ref 93. In fact, the $\{a_{ij}^{qq}, a_{ij}^{q\mu}, a_{ij}^{\mu\mu}\}$ parameters defining the width of the Gaussian damping for the ij interactions in ref 93 cannot be taken as independent (adjustable) parameters because they are linked through the Gaussian product rule,[94] i.e., $a_{ij}^{qq} = (a_{i_q}{}^2 + a_{j_q}{}^2)^{-0.5}$, $a_{ij}^{q\mu} = (a_{i_q}{}^2 + a_{j_\mu}{}^2)^{-0.5}$, and $a_{ij}^{\mu\mu} = (a_{i_\mu}{}^2 + a_{j_\mu}{}^2)^{-0.5}$, so that in general they are

dx.doi.org/10.1021/jp509074p | J. Phys. Chem. B 2014, 118, 13658−13670

tied by the relation $(a_{ij}^{q\mu})^2 = (a_{ij}^{qq})^2 + (a_{ij}^{\mu\mu})^2 - (a_{j_q}^{\ 2} + a_{j_\mu}^{\ 2})$. For example, the (a, b) Gaussian parameters in eqs 5 and 6 of ref 95 would (by definition) be identical to each other should the alleged formal equivalence be true because they are linked by the relation (if we follow the notation of ref 95) $f_2(r) = f_1(r) - r(\partial f_1(r)/\partial r)/3$ with $f_1 = \mathrm{erf}(r/a) - (2r/a\sqrt{\pi})\mathrm{e}^{-(r/a)^2}$ and $f_2 = f_1 - (4/3\sqrt{\pi})(r/a)^3\mathrm{e}^{-(r/a)^2}$ as given by A5-A7 of ref 93 after we invoke the identities $f_1 = s_1^{\mathrm{gau}}(r)$ and $f_2 = s_2^{\mathrm{gau}}(r)$. Therefore, the Hamiltonians underlying the GCP modeling and the point-based electrostatics with Gaussian damping functions describe two significantly different physical systems while attempting to overcome the same polarization phenomenon.

■ ASSOCIATED CONTENT

Supporting Information

Appendices that provide details on (A) the electrostatic interactions involving Gaussian charges and induced dipoles, (B) their real- and reciprocal-space contributions to the configurational energy and (C) virial in the Ewald implementation, (D) the long-range corrections to the nonelectrostatic contributions to the configurational energy and virial, and (E) the original reaction field version of the GCP modeling. This material is available free of charge via the Internet at http://pubs.acs.org.

■ AUTHOR INFORMATION

Corresponding Author

*E-mail: chialvoaa@ornl.gov. Fax: 865-574-4961.

Notes

The authors declare no competing financial interest.

■ ACKNOWLEDGMENTS

The authors are indebted to Drs. Gunnar Weck and Jon H. Eggert (Département de Physique Théorique et Appliquée CEA/DAM Ile de France) for providing the tabulated data from their X-ray diffraction experiments.[81] This research was supported by the Division of Chemical Sciences, Geosciences, and Biosciences, Office of Basic Energy Sciences, U.S. Department of Energy.

■ REFERENCES

(1) Guillot, B. A Reappraisal of What We Have Learnt During Three Decades of Computer Simulations on Water. *J. Mol. Liq.* **2002**, *101*, 219−260.

(2) Vega, C.; Abascal, J. L. F. Simulating Water with Rigid Non-Polarizable Models: A General Perspective. *Phys. Chem. Chem. Phys.* **2011**, *13*, 19663−19688.

(3) Jungwirth, P.; Tobias, D. J. Specific Ion Effects at the Air/Water Interface. *Chem. Rev.* **2006**, *106*, 1259−1281.

(4) Chang, T. M.; Dang, L. X. Recent Advances in Molecular Simulations of Ion Solvation at Liquid Interfaces. *Chem. Rev.* **2006**, *106*, 1305−1322.

(5) Zhu, S.-B.; Singh, S.; Robinson, G. W. Field-Perturbed Water. In *Modern Nonlinear Optics*; Evans, M., Kielich, S., Eds.; John Wiley & Sons, Inc.: New York, 1994; Vol. *85*, pp 627−732.

(6) Gregory, J. K.; Clary, D. C.; Liu, K.; Brown, M. G.; Saykally, R. J. The Water Dipole Moment in Water Clusters. *Science* **1997**, *275*, 814−817.

(7) Vlcek, L.; Chialvo, A. A.; Cole, D. R. Optimized Unlike-Pair Interactions for Water-Carbon Dioxide Mixtures Described by the SPC/E and EPM2 Models. *J. Phys. Chem. B* **2011**, *115*, 8775−8784.

(8) Chialvo, A. A.; Cummings, P. T. Molecular-Based Modeling of Water and Aqueous Solutions at Supercritical Conditions. In *Advances in Chemical Physics*; Rice, S. A., Ed.; Wiley & Sons: New York, 1999; Vol. *109*, pp 115−205.

(9) Halgren, T. A.; Damm, W. Polarizable Force Fields. *Curr. Opin. Struct. Biol.* **2001**, *11*, 236−242.

(10) Rick, S. W.; Stuart, S. J. Potentials and Algorithms for Incorporating Polarizability in Computer Simulations. In *Reviews in Computational Chemistry*; Lipkowitz, K. B., Boyd, D. B., Eds.; Wiley-VCH, Inc.: New York, 2002; Vol. *18*, pp 89−146.

(11) Cieplak, P.; Dupradeau, F. Y.; Duan, Y.; Wang, J. M. Polarization Effects in Molecular Mechanical Force Fields. *J. Phys.: Condens. Matter* **2009**, *21*, No. 333102.

(12) Svishchev, I. M.; Kusalik, P. G.; Wang, J.; Boyd, R. J. Polarizable Point-Charge Model of Water: Results under Normal and Extreme Conditions. *J. Chem. Phys.* **1996**, *105*, 4742−4750.

(13) Straatsma, T. P.; McCammon, J. A. Molecular Dynamics Simulations with Interaction Potentials Including Polarization Development of a Noniterative Method and Application to Water. *Mol. Simul.* **1990**, *5*, 181−192.

(14) Yu, H. B.; Hansson, T.; van Gunsteren, W. F. Development of a Simple, Self-Consistent Polarizable Model for Liquid Water. *J. Chem. Phys.* **2003**, *118*, 221−234.

(15) Lamoureux, G.; MacKerell, A. D.; Roux, B. A Simple Polarizable Model of Water Based on Classical Drude Oscillators. *J. Chem. Phys.* **2003**, *119*, 5185−5197.

(16) Kunz, A. P. E.; van Gunsteren, W. F. Development of a Nonlinear Classical Polarization Model for Liquid Water and Aqueous Solutions: COS/D. *J. Phys. Chem. A* **2009**, *113*, 11570−11579.

(17) Rappe, A. K.; Goddard, W. A. Charge Equilibration for Molecular-Dynamics Simulations. *J. Phys. Chem.* **1991**, *95*, 3358−3363.

(18) Rick, S. W.; Stuart, S. J.; Berne, B. J. Dynamical Fluctuating Charge Force Fields: Application to Liquid Water. *J. Chem. Phys.* **1994**, *101*, 6141−6156.

(19) Chen, B.; Xing, J.; Siepmann, J. I. Development of Polariable Water Force Fields for Phase Equilibrium Calculations. *J. Phys. Chem. B* **2000**, *104*, 2391−2401.

(20) Yu, H. B.; van Gunsteren, W. F. Accounting for Polarization in Molecular Simulation. *Comput. Phys. Commun.* **2005**, *172*, 69−85.

(21) Illingworth, C. J.; Domene, C. Many-Body Effects and Simulations of Potassium Channels. *Proc. R. Soc. A* **2009**, *465*, 1701−1716.

(22) Lopes, P. E. M.; Roux, B.; MacKerell, A. D. Molecular Modeling and Dynamics Studies with Explicit Inclusion of Electronic Polarizability: Theory and Applications. *Theor. Chem. Acc.* **2009**, *124*, 11−28.

(23) Alfredsson, M.; Brodholt, J. P.; Hermanson, K.; Vallauri, R. The Use of a Point Polarizable Dipole in Intermolecular Potentials for Water. *Mol. Phys.* **1998**, *94*, 873−876.

(24) Piquemal, J. P.; Chelli, R.; Procacci, P.; Gresh, N. Key Role of the Polarization Anisotropy of Water in Modeling Classical Polarizable Force Fields. *J. Phys. Chem. A* **2007**, *111*, 8170−8176.

(25) Böttcher, C. J. F. *Theory of Electric Polarization*; Elsevier: Amsterdam, The Netherlands, 1973; Vol. *1*.

(26) Soderhjelm, P.; Ohrn, A.; Ryde, U.; Karlstrom, G. Accuracy of Typical Approximations in Classical Models of Intermolecular Polarization. *J. Chem. Phys.* **2008**, *128*, No. 014102.

(27) Thole, B. T. Molecular Polarizabilities Calculated with a Modified Dipole Interaction. *Chem. Phys.* **1981**, *59*, 341−350.

(28) Bernardo, D. N.; Ding, Y.; Krogh-Jespersen, K. An Anisotropic Polarizable Water Model: Incorporation of All-Atom Polarizabilities into Molecular Mechanics Force Fields. *J. Phys. Chem.* **1994**, *98*, 4180−4187.

(29) Chialvo, A. A.; Cummings, P. T. Simple Transferable Intermolecular Potential for the Molecular Simulation of Water over Wide Ranges of State Conditions. *Fluid Phase Equilib.* **1998**, *150−151*, 73−81.

(30) Chelli, R.; Procacci, P.; Transferable, A. Polarizable Electrostatic Force Field for Molecular Mechanics Based on the Chemical Potential Equalization Principle. *J. Chem. Phys.* **2002**, *117*, 9175−9189.

(31) Paricaud, P.; Predota, M.; Chialvo, A. A.; Cummings, P. T. From Dimer to Condensed Phases at Extreme Conditions: Accurate Predictions of the Properties of Water by a Gaussian Charge Polarizable Model. *J. Chem. Phys.* **2005**, *122*, 244511.
(32) Baranyai, A.; Kiss, P. T. A Transferable Classical Potential for the Water Molecule. *J. Chem. Phys.* **2010**, *133*, No. 144109.
(33) Ren, P. Y.; Ponder, J. W. Polarizable Atomic Multipole Water Model for Molecular Mechanics Simulation. *J. Phys. Chem. B* **2003**, *107*, 5933−5947.
(34) Masia, M.; Probst, M.; Rey, R. On the Performance of Molecular Polarization Methods. II. Water and Carbon Tetrachloride Close to a Cation. *J. Chem. Phys.* **2005**, *123*, No. 164505.
(35) Sprik, M.; Klein, M. L. A Polarizable Model for Water Using Distributed Charge Sites. *J. Chem. Phys.* **1988**, *89*, 7556−7560.
(36) Zhu, S.-B.; Singh, S.; Robinson, G. W. A New Flexible/Polarizable Water Model. *J. Chem. Phys.* **1991**, *95*, 2791−2799.
(37) Kolafa, J.; Moucka, F.; Nezbeda, I. Handling Electrostatic Interactions in Molecular Simulations: A Systematic Study. *Collect. Czech. Chem. Commun.* **2008**, *73*, 481−506.
(38) Adams, D. J.; Adams, E. M.; Hills, G. J. Computer-Simulation of Polar Liquids. *Mol. Phys.* **1979**, *38*, 387−400.
(39) Wolf, D.; Keblinski, P.; Phillpot, S. R.; Eggebrecht, J. Exact Method for the Simulation of Coulombic Systems by Spherically Truncated, Pairwise R(−1) Summation. *J. Chem. Phys.* **1999**, *110*, 8254−8282.
(40) Fennell, C. J.; Gezelter, J. D. Is the Ewald Summation Still Necessary? Pairwise Alternatives to the Accepted Standard for Long-Range Electrostatics. *J. Chem. Phys.* **2006**, *124*, No. 234104.
(41) Adams, D. J.; Dubey, G. S. Taming the Ewald Sum in the Computer Simulation of Charged Systems. *J. Comput. Phys.* **1987**, *72*, 156−176.
(42) Steinhauser, O. Reaction Field Simulation of Water. *Mol. Phys.* **1982**, *45*, 335−348.
(43) Hummer, G.; Soumpasis, D. M. Computation of the Water Density Distribution at the Ice-Water Interface Using the Potentials-of-Mean-Force Expansion. *Phys. Rev. E* **1994**, *49*, 591−596.
(44) de Leeuw, S. W.; Perram, J. W.; Smith, E. R. Simulation of Electrostatic Systems in Periodic Boundary-Conditions 0.1. Lattice Sums and Dielectric-Constants. *Proc. R. Soc. London, Ser. A* **1980**, *373*, 27−56.
(45) Sperb, R. Extension and Simple Proof of Lekner Summation Formula for Coulomb Forces. *Mol. Simul.* **1994**, *13*, 189−193.
(46) Mazars, M. Electroneutrality in the Lekner-Sperb Method. *Mol. Phys.* **2005**, *103*, 675−678.
(47) Schoen, M.; Klapp, S. H. L. *Nanoconfined Fluids. Soft Matter between Two and Three Dimensions*; John Wiley & Sons: Hoboken, NJ, 2007; Vol. *24*, pp 447−478.
(48) Ruocco, G.; Sampoli, M. Computer-Simulation of Polarizable Fluids - a Consistent and Fast Way for Dealing with Polarizability and Hyperpolarizability. *Mol. Phys.* **1994**, *82*, 875−886.
(49) Chialvo, A. A.; Cummings, P. T. Engineering a Simple Polarizable Model for the Molecular Simulation of Water Applicable over Wide Ranges of State Conditions. *J. Chem. Phys.* **1996**, *105*, 8274−8281.
(50) Chialvo, A. A.; Cummings, P. T. Molecular-Based Modeling of Water and Aqueous Solutions at Supercritical Conditions. *Advances in Chemical Physics*; John Wiley & Sons, Inc.: New York, 1999; pp 115−205.
(51) Postorino, P.; Ricci, M. A.; Soper, A. K. Water above Its Boiling Point: Study of the Temperature and Density Dependence of the Partial Pair Correlation Functions. I. Neutron Diffraction Experiment. *J. Chem. Phys.* **1994**, *101*, 4123−4132.
(52) Tromp, R. H.; Postorino, P.; Neilson, G. W.; Ricci, M. A.; Soper, A. K. Neutron-Diffraction Studies of H2o/D2o at Supercritical Temperatures - a Direct Determination of G(HH)(r) G(OH)(r), and G(OO)(r). *J. Chem. Phys.* **1994**, *101*, 6210−6215.
(53) Soper, A. K.; Bruni, F.; Ricci, M. A. Site-Site Pair Correlation Functions of Water from 25°C to 400°C: Revised Analysis of New and Old Diffraction Data. *J. Chem. Phys.* **1997**, *106*, 247−254.
(54) Benjamin, K. M.; Schultz, A. J.; Kofke, D. A. Virial Coefficients of Polarizable Water: Applications to Thermodynamic Properties and Molecular Clustering. *J. Phys. Chem. C* **2007**, *111*, 16021−16027.
(55) Benjamin, K. M.; Schultz, A. J.; Kofke, D. A. Fourth and Fifth Virial Coefficients of Polarizable Water. *J. Phys. Chem. B* **2009**, *113*, 7810−7815.
(56) Kiss, P. T.; Baranyai, A. Clusters of Classical Water Models. *J. Chem. Phys.* **2009**, *131*, No. 204310.
(57) Rivera, J. L.; Starr, F. W.; Paricaud, P.; Cummings, P. T. Polarizable Contributions to the Surface Tension of Liquid Water. *J. Chem. Phys.* **2006**, *125*, No. 094712.
(58) Chialvo, A. A.; Horita, J. Polarization Behavior of Water in Extreme Aqueous Environments: A Molecular Dynamics Study Based on the Gaussian Charge Polarizable Water Model. *J. Chem. Phys.* **2010**, *133*, No. 074504.
(59) Hirschfelder, J. O.; Curtiss, C. F.; Bird, R. B. *Molecular Theory of Gases and Liquids*; John Wiley & Sons, Inc.: New York, 1954.
(60) Chialvo, A. A.; Horita, J. Liquid-Vapor Equilibrium Isotopic Fractionation of Water: How Well Can Classical Water Models Predict It? *J. Chem. Phys.* **2009**, *130*, No. 094509.
(61) Ahlström, P.; Wallqvist, A.; Engström, S.; Jönsson, B. A Molecular Dynamics Study of Polarizable Water. *Mol. Phys.* **1989**, *68*, 563−581.
(62) Chelli, R.; Righini, R.; Califano, S.; Procacci, P. Towards a Polarizable Force Field for Molecular Liquids. *J. Mol. Liq.* **2002**, *96*−*7*, 87−100.
(63) Abramowitz, M.; Stegun, I. A. *Handbook of Mathernatical Functions*; Dover: New York, 1965.
(64) Vesely, F. J. N-Particle Dynamics of Polariable Stockmayer-Type Molecules. *J. Comput. Phys.* **1977**, *24*, 361−371.
(65) Feller, S. E.; Pastor, R. W.; Rojnuckarin, A.; Bogusz, S.; Brooks, B. R. Effect of Electrostatic Force Truncation on Interfacial and Transport Properties of Water. *J. Phys. Chem.* **1996**, *100*, 17011−17020.
(66) Spohr, E. Effect of Electrostatic Boundary Conditions and System Size on the Interfacial Properties of Water and Aqueous Solutions. *J. Chem. Phys.* **1997**, *107*, 6342−6348.
(67) Baumketner, A. Removing Systematic Errors in Interionic Potentials of Mean Force Computed in Molecular Simulations Using Reaction-Field-Based Electrostatics. *J. Chem. Phys.* **2009**, *130*, No. 104106.
(68) Cisneros, G. A.; Karttunen, M.; Ren, P.; Sagui, C. Classical Electrostatics for Biomolecular Simulations. *Chem. Rev.* **2014**, *114*, 779−814.
(69) This condition allows the simultaneous convergence of the short-range interactions in the real space and the long-range interactions in the reciprocal space. Otherwise, the entire calculation must be done in the reciprocal space.
(70) Boys, S. F. Electronic Wave Functions 0.1. A General Method of Calculation for the Stationary States of Any Molecular System. *Proc. R. Soc. London, Ser. A* **1950**, *200*, 542−554.
(71) Helgaker, T.; Jørgensen, P.; Olsen, J. *Molecular Electronic Structure Theory*; Wiley: Chichester, U.K., 2000.
(72) Nymand, T. M.; Linse, P. Ewald Summation and Reaction Field Methods for Potentials with Atomic Charges, Dipoles, and Polarizabilities. *J. Chem. Phys.* **2000**, *112*, 6152−6160.
(73) Jeon, J.; Lefohn, A. E.; Voth, G. A. An Improved Polarflex Water Model. *J. Chem. Phys.* **2003**, *118*, 7504−7518.
(74) Aguado, A.; Madden, P. A. Ewald Summation of Electrostatic Multipole Interactions up to the Quadrupolar Level. *J. Chem. Phys.* **2003**, *119*, 7471−7483.
(75) Stenhammar, J.; Trulsson, M.; Linse, P. Some Comments and Corrections Regarding the Calculation of Electrostatic Potential Derivatives Using the Ewald Summation Technique. *J. Chem. Phys.* **2011**, *134*, No. 224104.
(76) Hill, T. L. *Statistical Mechanics: Principles and Selected Applications*; McGraw-Hill: New York, 1956.
(77) Andersen, H. C. Molecular Simulations at Constant Pressure and/or Temperature. *J. Chem. Phys.* **1980**, *72*, 2384−2393.

(78) Nosé, S. A Unified Formulation of the Constant Temperature Molecular Dynamics Methods. *J. Chem. Phys.* **1984**, *81*, 511−519.
(79) Nosé, S. A Molecular Dynamics Method for Simulations in the Canonical Ensemble. *Mol. Phys.* **1984**, *52*, 255−268.
(80) Soper, A. K. The Radial Distribution Functions of Water and Ice from 220 to 673 K and at Pressures up to 400 MPa. *Chem. Phys.* **2000**, *258*, 121−137.
(81) Weck, G.; Eggert, J.; Loubeyre, P.; Desbiens, N.; Bourasseau, E.; Maillet, J. B.; Mezouar, M.; Hanfland, M. Phase Diagrams and Isotopic Effects of Normal and Deuterated Water Studied Via X-Ray Diffraction up to 4.5 GPa and 500 K. *Phys. Rev. B* **2009**, *80*, No. 180202.
(82) Sanchez-Valle, C.; Mantegazzi, D.; Bass, J. D.; Reusser, E. Equation of State, Refractive Index and Polarizability of Compressed Water to 7 GPa and 673 K. *J. Chem. Phys.* **2013**, *138*, No. 054505.
(83) Gear, C. W. *The Numerical Integration of Ordinary Differential Equations of Various Orders*; ANL-7126; Argonne National Laboratory: Chicago, IL, 1966.
(84) Evans, D. J.; Murad, S. Singularity Free Algorithm for Molecular Dynamics Simulation of Rigid Polyatomics. *Mol. Phys.* **1977**, *34*, 327−331.
(85) Flyvbjerg, H.; Petersen, H. G. Error-Estimates on Averages of Correlated Data. *J. Chem. Phys.* **1989**, *91*, 461−466.
(86) Kolafa, J. Time-Reversible Always Stable Predictor-Corrector Method for Molecular Dynamics of Polarizable Molecules. *J. Comput. Chem.* **2004**, *25*, 335−342.
(87) Skinner, L. B.; Huang, C.; Schlesinger, D.; Pettersson, L. G. M.; Nilsson, A.; Benmore, C. J. Benchmark Oxygen-Oxygen Pair-Distribution Function of Ambient Water from X-Ray Diffraction Measurements with a Wide Q-Range. *J. Chem. Phys.* **2013**, *138*, No. 074506.
(88) Neumann, M. Dipole Moment Fluctuation Formulas in Computer Simulations of Polar Systems. *Mol. Phys.* **1983**, *50*, 841−858.
(89) Schreiber, H.; Steinhauser, O. Molecular-Dynamics Studies of Solvated Polypeptides - Why the Cutoff Scheme Does Not Work. *Chem. Phys.* **1992**, *168*, 75−89.
(90) Hunenberger, P. H.; van Gunsteren, W. F. Alternative Schemes for the Inclusion of a Reaction-Field Correction into Molecular Dynamics Simulations: Influence on the Simulated Energetic, Structural, and Dielectric Properties of Liquid Water. *J. Chem. Phys.* **1998**, *108*, 6117−6134.
(91) English, N. J. Molecular Dynamics Simulations of Liquid Water Using Various Long Range Electrostatics Techniques. *Mol. Phys.* **2005**, *103*, 1945−1960.
(92) Fulton, J. L.; Schenter, G. K.; Baer, M. D.; Mundy, C. J.; Dang, L. X.; Balasubramanian, M. Probing the Hydration Structure of Polarizable Halides: A Multiedge Xafs and Molecular Dynamics Study of the Iodide Anion. *J. Phys. Chem. B* **2010**, *114*, 12926−12937.
(93) Sala, J.; Guardia, E.; Masia, M. The Polarizable Point Dipoles Method with Electrostatic Damping: Implementation on a Model System. *J. Chem. Phys.* **2010**, *133*, No. 234101.
(94) Shavitt, I. The Gaussian Function in Calculations of Statistical Mechanics and Quantum Mechanics. In *Methods in Computational Physics*; Alder, B., Fernbach, S., Rotenberg, M., Eds.; Academic Press: New York, 1963; Vol. 2, pp 1−45.
(95) Masia, M.; Probst, M.; Rey, R. Polarization Damping in Halide-Water Dimers. *Chem. Phys. Lett.* **2006**, *420*, 267−270.